BNL-223483-2022-JAAM

Phasing Magnet for CSX-2 beamline at NSLS-II

M. Musardo

To be published in "IEEE Xplore"

March 2022

Photon Sciences

Brookhaven National Laboratory

U.S. Department of Energy

USDOE Office of Science (SC), Basic Energy Sciences (BES) (SC-22)

DISCLAIMER

Phasing Magnet for CSX-2 beamline at NSLS-II

M. Musardo, T. Tanabe, J. Rank, D. Harder, T. Corwin, and C. Rhein,
Photon Science Directorate, Brookhaven National Laboratory, Upton, NY, 11973 U.S.A.

***Abstract*—A phasing magnet has been developed at National Synchrotron Light Source II (NSLS-II) for the Coherent Soft X-ray Scattering (CSX) beamline. The phasing magnet will be located at the center of the straight section in between two identical and independent variably polarized APPLE-II devices. Based on Permanent Magnet technology, the phasing magnet has been designed to achieve the required electron beam delay to properly adjust the phase matching of these two consecutive EPUs (Elliptically Polarizing Undulators) and ensure a positive interference between the photon beam emitted in each device. This paper will describe the mechanical and magnetic design together with the final field measurements and magnetic tuning results. Also, the spectral performance of the two EPUs and the method used to properly set the field strength of the phasing magnet for any given radiation wavelength and polarization mode will be presented as well.**

***Index Terms*—Undulator, synchrotron light source, synchrotron radiation, magnetic measurement.**

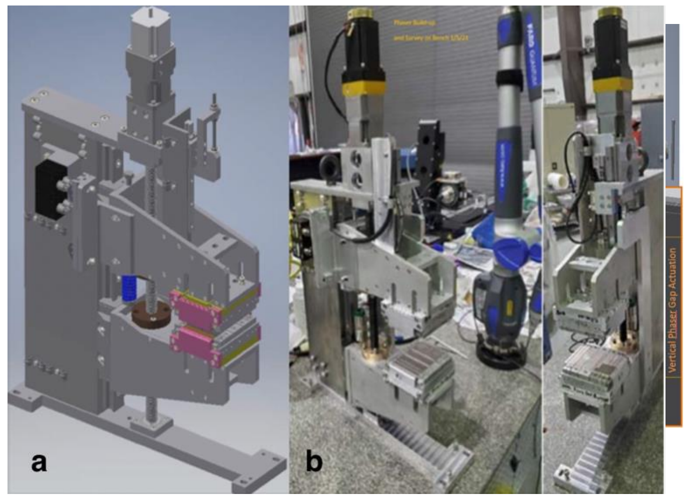

I. Introduction

HISTORICALLY the National Synchrotron Light Source II Coherent Soft X-ray Scattering canted beamlines at C23 (NSLS-II CSX and IOS, formerly CSX-1&2) were independently sourced via two identical variably polarized APPLE-II EPU49 devices. Limited phasing could only be crudely achieved by shift of the four independent longitudinal axes of each EPU. Maximum brightness by positive interference of beams from each EPU was not achievable.

This paper describes the mechanical and magnetic designs of the NSLS-II CSX-2 Phaser. It further gives the final field measurements and magnetic tuning results along with the spectral performance of the two EPU and the method used to properly set the field strength of the Phaser for any given radiation wavelength and polarization mode. The development of an interstitial Phasing Magnet (Phaser hereafter, shown Figure 1) was undertaken to bring improved performance to CSX-2 users with more intense light from an effective 4.0-meter source with improved phasing control by adjusting electron path length [1]. This Phaser now installed in the very narrow space downstream of the existing Canting Magnet shares its stanchion and a channel from its motor driver and controls as shown in Figure 2.

II. Overall Objectives of Phaser Mechanical design

The Phaser structure and magnet core must accommodate the wide "Dog Bone" cross-section of the existing vacuum chamber with its deep recessed pocket which allows for minimized magnetic gap (Figure 3). This requires: 1) a deep throated design of the Phaser "jaws" (thus large bending moment as the chamber edge is near to the actuated vertical axis), and 2) no core structure permitted inside of its magnet plane. Terminal permanent

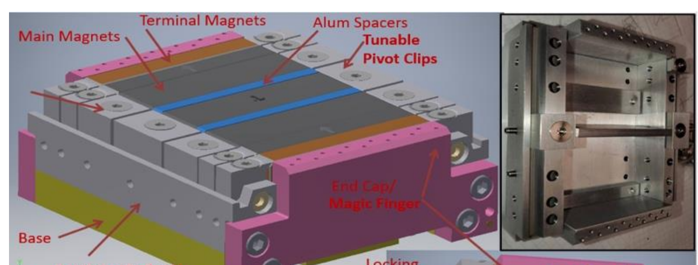

Fig 2. Phaser integrated into canted straight; Inset: Canting Magnet and Phaser within interstitial space.

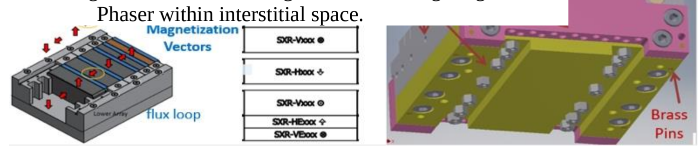

Manuscript receipt and acceptance dates will be inserted here. This work was supported by DOE under contract DE-SC0012704. *(Corresponding author: Marco Musardo.)*

The authors are with the Energy and Photon Sciences Directorate, NSLS-II, Brookhaven National Laboratory, Upton, NY 11973 USA (e-mail: musardo@bnl.gov).

Color versions of one or more of the figures in this paper are available online at http://ieeexplore.ieee.org.

Digital Object Identifier will be inserted here upon acceptance.

magnets are stacked face to face. Additionally, for tuning capability we require a set of Magic Finger Assemblies (MF) at both ends further consuming the available longitudinal space. The shortest possible magnetic length was achieved by integration of the MF into core end. Upstream, the proximity to the existing Canting Magnet (CM), and downstream to the EPU-2 when extended to half lambda phase, requires careful consideration of mutual magnetic interaction. For alignment with electron beam an independent means of elevation adjustment from that of the CM is included. Finally, for commonality and interchangeability the design makes use of NSLS-II and ID standard, inventoried hardware (step motor, absolute encoder and scale length, position switches, shielding, etc.).

III. Mechanical Design of the Phaser Core

Four types of custom permanent magnets (PM) of varying length and magnetization construct the Phaser Magnet Core depicted in Figure 4. These are of the N41UHR grade of Neodymium-Iron-Boron rare earth magnet having 25 kOe intrinsic coercivity and are oven-aged and nickel plated. Each underwent

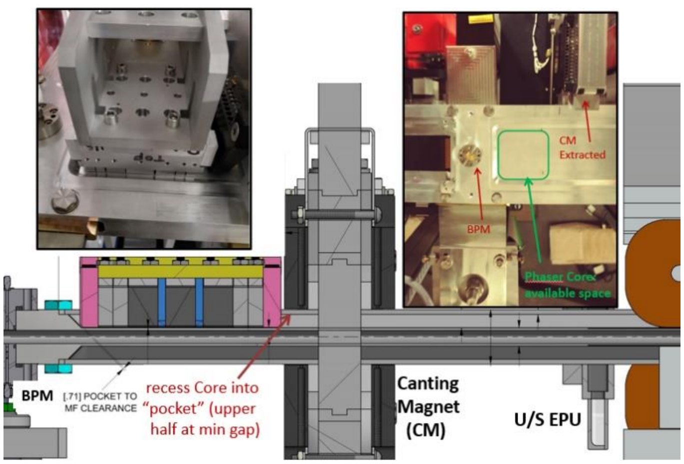

Fig. 3. Section through chamber 'pocket' at closed gap; Inset**:** Existing ring constraint isometric and plan photos.

magnetic characterization for PM sorting in our Helmholtz coil while fixtured in a custom 3D-printed measurement fixture (inset, Figure 5). The PM array has design features which allow for expanded tuning capacity [2]. These are depicted in Figure 5 as: 1) pivoting PM retaining clips fastened by a system of cross-threaded cylinders, or dowels (two per PM); and 2) side and bottom set screw adjustors, and 3) MF pill-capturing set screws with integral spacer of varying lengths (SHSS). Stress analyses were performed on core components, and a 2.4kN (30"-lb torque) proof test conducted on the titanium dowels (Ti-6Al-4V) to confirm their integrity, as presented in the inset of Figure 5. Advantages of the cross-dowel design include pivot for increase rotation and translation DOF of individual PM; flexibility in control of periodicity; increased strength compared with aluminum taps; and a single through-bore replacing many tapped holes thereby lowering cost.

IV. Mechanical and Structural Assembly of Phaser

The Phaser mechanics is single axis consisting of a ¾"-6 ACME right-hand left-hand (RH/LH) lead screw. The screw is non-lubricated and acts on two opposing nuts from C932 bronze (ASTM B148 C93200). These actuate the gap through a flexible-coupled step motor with 1.21 N-m peak torque output rating driving a 20:1 gearhead. The full-speed ramp up takes 1 second.

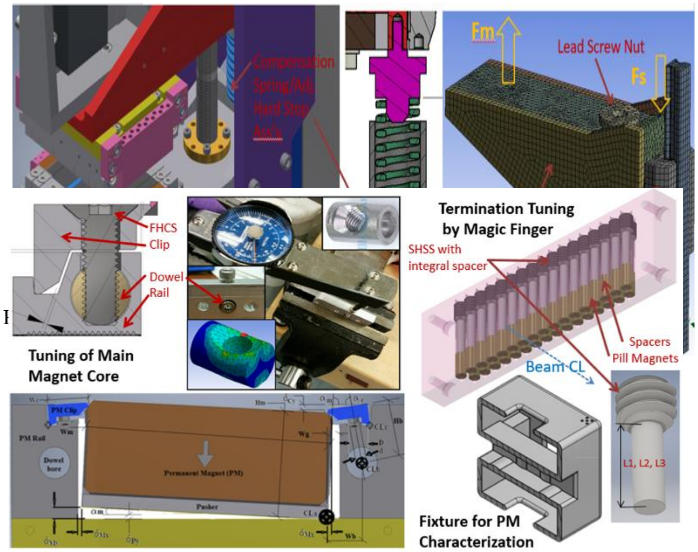

The nuts which are nearest to both gap and electron beam have low relative magnetic permeability (< 1.3). The lead screw, however, is from high permeability hardened steel. The calculated fringe field at 115 mm is acceptable 15 G. The drive axis is self-locking to inhibit overhaul without a brake. A single sub-assembly serves both as spring compensation system and as a finely adjustable hard stop. Gravitational force acting on the RH/LH screw self-cancels. A heavy die spring opposes magnetic force at small gaps. Critically, at all gaps the design assures a positive net load to inhibit backlash with smooth axis motion. Lifetime calculations for the bronze nuts yield acceptable PV value with good wear characteristics. The "jaws" they drive are each supported by a linear bearing and rail system (THK P/N SRG30XLC2SSC0+460LSPZ) with high stiffness to resist the large bending moment. Refer to the right of Figure 6. The lead screw design has appropriate JIS B 0401-1 class fits for ball bearing supports at each end. At the motor end a self-aligning ball bearing (SKF 2201 E-2RS1TN9) is of tolerance class J5. At the base an angular contact bearing (FAG 7201) is of tolerance class K6. The radiation sensitive electronic absolute encoder/scale providing positional feedback is shielded by lead.

V. Magnetic Design of Phaser

The device's magnetic length is 99.0 mm, and the minimum operational gap is 15 mm, the magnet height/width is 25 mm and 66 mm respectively. The magnet thickness is 18 mm and 4.5 mm spacings on both sides of the center magnet. All magnets have 2 mm chamfer at four corners. Figure 7 shows the magnetic model's rendering by Mathematica [3] and the associate vertical magnetic field profile at 15 mm of gap.

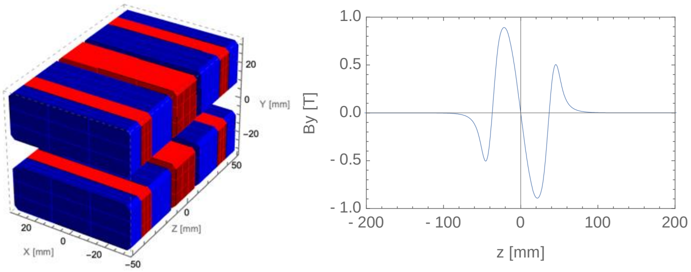

Fig. 7: 3D magnetic model and vertical magnetic field profile at 15 mm of gap.

The remanence of the magnet is 1.2 T and the standard susceptibility values are used into the Radia simulation [4, 5]. The magnetic structure is composed of 14 NdFeB blocks arranged in an undulator-like configuration and low fringe-field terminations are used to reduce the magnetic crosstalk among the adjacent EPUs.

VI. Magnetic Measurements and Tuning

The Phaser has been characterized by Hall probe and Flip-Coil measurements to determinate the magnetic field distribution (Figure 8), the field integrals (Figure 9), the integrated multipole (inset, Figure 9), and the phase integral (Figure 10) along the device for different gaps. The maximum value of the phase integral measured at the minimum gap of 15 mm is 5941 T^2mm^3 as shown in Figure 11. The vertical and horizontal field integrals measured before and after magnetic tuning are shown in the Figure 12. The magnetic optimization was achieved by an arrangement of small cylindrical permanent magnet blocks called Magic Finger inserted into special holders and mounted to both ends of the upper and lower magnet arrays of the Phaser. The Magic Finger optimization was carried out using “IDBuilder”, a genetic algorithm-based computer code for magnetic tuning of undulators [6, 7].

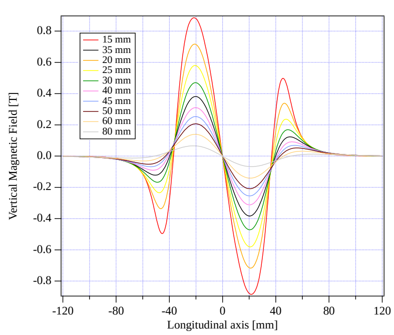

Fig. 8: On-axis vertical magnetic field at different gaps.

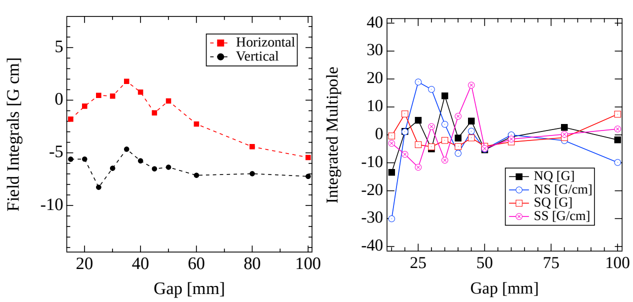

Fig. 9: Field integral components and integrated multipole at different gaps.

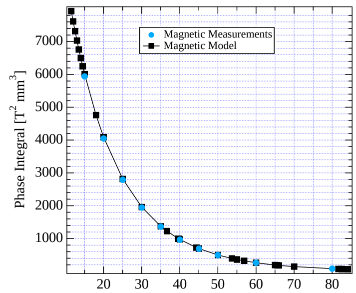

Fig. 10: Phase Integral measured and calculated at different gaps.

To achieve phase matching between the two EPUs a numerical calculation is necessary to predict the required phase delay. The phase change is calculated by determining the slippage between the two devices, which is determined by their physical separation, gap, and array shift (phase). The electron beam must keep a proper phase relationship with the radiation for any given radiation wavelength λ and polarization mode to reach a constructive interference between the two EPUs. The relative phase of an electron with respect to the radiation is expressed by the optical phase function [8, 9]:

$$\psi(z) = \frac{2\pi}{\lambda}\left(\frac{z}{2\gamma^2} + \frac{1}{2}\int_{-\infty}^{z} x'^2(z')dz'\right) \quad (1)$$

Here, z is the coordinate along the beam path, γ is the Lorentz factor and x' is the deflection angle of the electron, which is derived from the magnetic field distribution B(z) along the longitudinal axis of the device:

$$x'(z) = -\frac{e}{\gamma mc}\int_{-\infty}^{z} B(z')\,dz' \quad (2)$$

where e is the electron charge, m its rest mass and c is the speed of light. The first term of the Eq. 1 describes the phase advance in the drift space, while the second term represents the contribution of the magnetic field. By means of equation (1) and (2) the optical phase can be evaluated from the measured magnetic field data. The phase advance can ben written as:

$$\Delta\psi(z) = \frac{2\pi}{\lambda_u\left(1+\frac{K^2}{2}\right)}\left(\frac{e}{mc}\right)^2 \left\{\int_{-\infty}^{z}\left(\int_{-\infty}^{z''} B(z')dz'\right)^2 dz''\right\} \quad (3)$$

where K and λ_u are the deflection parameter and the undulator period length, respectively. The phase delay required to properly tune the phase matching of these two consecutive EPUs can be adjusted by adjusting the K value. Therefore, the magnetic field of the Phaser must be set in order that the phase difference between the centers of the two devices for a particular radiation wavelength and polarization mode reaches an integer multiple of 2π, corresponding to a constructive interference between the two sources. In practice, only the total phase shift of the device is of interest, which is obtained from Eq. 3 by extending the integration to +∞. The expression in the curled brackets is commonly called phase integral (PI) and it is defined as:

$$PI = \int_{-\infty}^{+\infty} \left(\int_{-\infty}^{z''} B(z')dz' \right)^2 dz'' \quad (4)$$

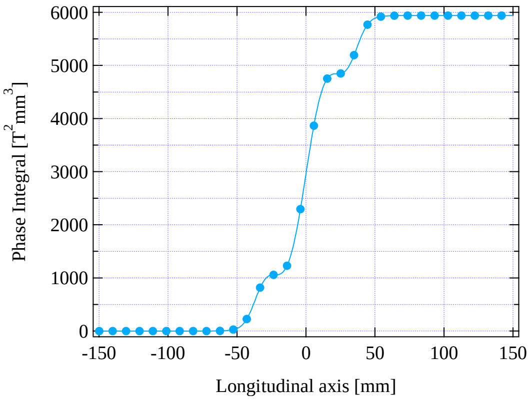

Fig. 11: Phase Integral at 15 mm gap.

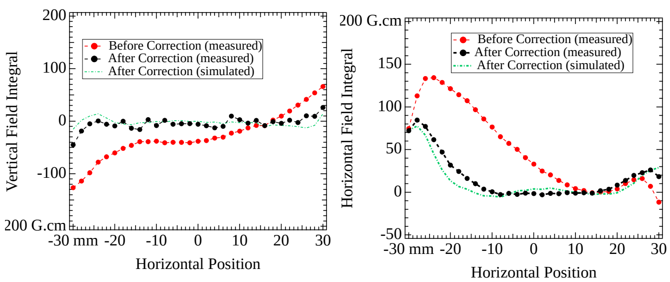

Fig. 12: Vertical and horizontal residual field integral before (red dots) and after (black dots) magnetic tuning and comparison between the final measurement (black dots) and the field integral simulated (green dots).

The effect of the Phaser on the spectral performance of the two EPUs in series has been investigated at different polarization mode and for specific harmonic, several spectrum simulations have been made based on magnetic measurements. A clear constructive interference pattern is visible in the flux density in the Figure 13 at a photon energy of 931.5 eV.

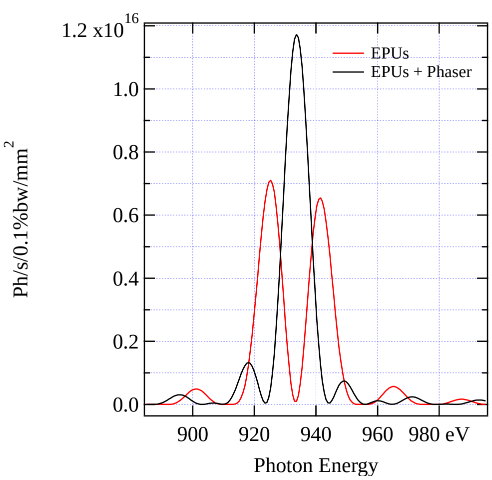

Fig. 13: On-axis flux density of the two EPUs in circular polarization with and without the Phaser.

VII. Conclusion

The restrictive physical constraints of the interstitial space between two tandem canted EPU49 at the C23 straight section of the NSLS-II ring have been overcome by design of a unique Phaser magnet core and structure. The magnet core design is highly bench-tunable, and the mechanics employ a versatile compensation system to permit use of our most common and interchangeable NSLS-II ID components. Magnetic measurements by Hall Probe and Flip-Coil were performed and met specification with minimal tuning. The Phaser now in service provides efficient phasing control for an effective 4.0-meter source to the CSX-2 beamline users.

References

[1] T. Tanabe, et. al., BNL; SLAC prototype magnet SA-381-921-75

[2] J. Rank, BNL; C23 Phaser Design Review, 10/4/20

[3] Mathematica is a registered trademark of Wolfram Research, Inc.

[4] O. Chubar, P. Elleaume and J. Chavanne, A 3D Magnetostatics Computer Code for Insertion Devices, Journal of Synchrotron Radiation, 1998, vol.5, pp.481-484.

[5] O. Chubar, et. Al.," Parametric Optimization of Undulators for NSLS-II Project Beamlines", SRI-2009, AIP Conference Proceedings Vol. 1234, pp.37-40.

[6] O. Chubar, "Application of Genetic Algorithms to Sorting, Swapping and Shimming of the SOLEIL Undulator magnets", SRI-2006, AIP Conf. Proc. vol. 879, pp.359-362

[7] O. Rudenko and O. Chubar, "An Evolutionary Approach to Shimming Undulator Magnets for Synchrotron Radiation Sources", Proc. PPSN IX, 2006.

[8] B. Diviacco and R. P. Walker, "The effect of magnetic field errors on the radiation spectrum of ELETTRA undulators. Proc. IPAC89, Chicago, pp. 1259-1261.

[9] R. P. Walker, "Interference effects in undulator and wiggler radiation sources", Nucl. Instrum. Methods, A335:328-337, 1993